Applying Deep Learning to Anomaly Detection of Russian Satellite Activity for Indications Prior to Military Activity

David Kurtenbach
Kansas State University
Megan Manly
Kansas State University

Zach Metzinger
Kansas State University

ABSTRACT

We apply deep learning techniques for anomaly detection to analyze activity of Russian-owned resident space objects (RSO) prior to the Ukraine invasion and assess the results for any findings that can be used as indications and warnings (I&W) of aggressive military behavior for future conflicts. Through analysis of anomalous activity, an understanding of possible tactics and procedures can be established to assess the existence of statistically significant changes in Russian RSO pattern of life/pattern of behavior (PoL/PoB) using publicly available two-line element (TLE) data. This research looks at statistical and deep learning approaches to assess anomalous activity. The deep learning methods assessed are isolation forest (IF), traditional autoencoder (AE), variational autoencoder (VAE), Kolmogorov Arnold Network (KAN), and a novel anchor-loss based autoencoder (Anchor AE). Each model is used to establish a baseline of on-orbit activity based on a five-year data sample. The primary investigation period focuses on the six months leading up to the invasion date of February 24, 2022. Additional analysis looks at RSO activity during an active combat period by sampling TLE data after the invasion date. The deep learning autoencoder models identify anomalies based on reconstruction errors that surpass a threshold sigma. To capture the nuance and unique characteristics of each RSO an individual model was trained for each observed space object. The total number of models trained and used for inference is 2,544 which is based on a select number of space objects that met the defined criteria to be included in the research. The research made an effort to prioritize explainability and interpretability of the model results thus each observation was assessed for anomalous behavior of the individual six orbital elements versus analyzing the input data as a single monolithic observation. The results demonstrate not only statistically significant anomalies of Russian RSO activity but also details anomalous findings to the individual orbital element. To drive explainability, objects were analyzed based on their categorized mission class. This helps create understandable results that can be extended to establish a generalized profile of space operations leading up to aggressive military actions. The codebase is available at https://github.com/davidkurtenb/Russat_AnomDetect

1. INTRODUCTION

There is an ever-growing dependency and importance placed on space-based assets and the capabilities they provide. Satellites are critical in providing important functionality that ranges from communication, data transfer, and weather analysis. As dependencies on space-based capabilities continue to increase, so does the support of these capabilities in military activities and their importance to warfighting. They enable secure communications, collect and deliver intelligence, and provide the capability to employ advanced weapon systems [8]. Employing space-based effects to support terrestrial military campaigns requires considerable planning and time to execute, particularly for space objects in a GEO. As space technologies continue to expand in applications for civilian and military benefits, the need to detect and establish robust PoLs/PoBs becomes ever more pertinent. Detecting and understanding subtle changes in a given RSO's on-orbit behavior offers potential insight to future intent. As more complex analysis is performed to look beyond a single RSO's PoL/PoB and to analyze across multiple RSOs, there is an opportunity to establish profiles of tactics and procedures of space-operating nations. TLE data captures a space object's behaviors and, when

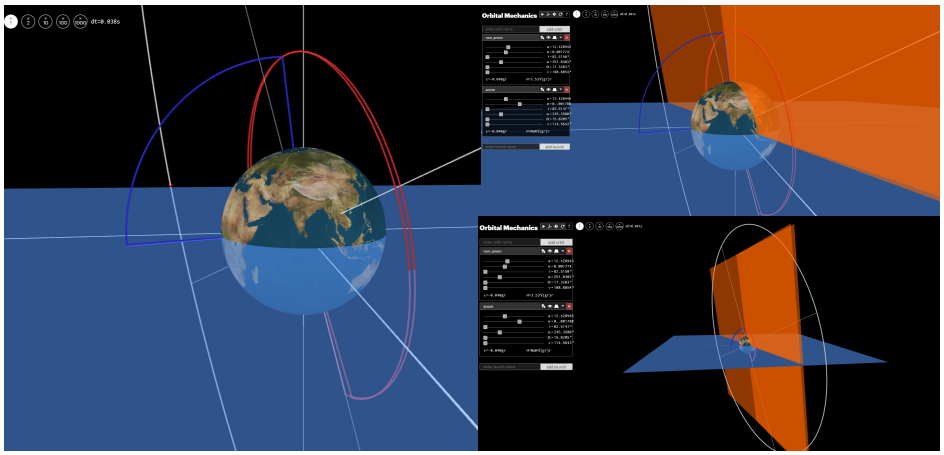

Fig. 1: Changes in orbital plane between propagated orbit of last non-anomalous observation compared to post anomaly orbit of a selected RSO.

used as training data for a machine learning model, may allow the model to identify specific actions that violate an established PoL/PoB. It provides a means to quickly assess vast amounts of data and identify particular activities that can be an indication of ongoing military action. As the number of objects in space grows along with the number of sensor networks, the amount of data collected only stands to increase. The volume of data currently collected exceeds the amount that can be manually processed at a reasonable rate of quality and efficiency. Leveraging advanced data science techniques has been effective in quickly analyzing vast amounts of data, but there is a growing need to do it faster and at lower computational costs. A prominent test case for military wartime action by a spacefaring country is the Russian invasion of Ukraine. Using verbose publicly available data sources, deep learning techniques can be applied to identify behavioral changes of space objects to provide potential I&W of oncoming adversarial actions. This project investigated and analyzed Russian-owned RSO activity prior to the invasion of Ukraine on February 24, 2022 using publicly available TLE data sourced from Space-Track.org [2]. The research looked at the six classical orbital elements of Russian RSOs for use in deep learning algorithms to assess and detect anomalous activity. An anchor-loss autoencoder was developed and compared alongside other deep learning methodologies to identify anomalies and establish a profile of pre-conflict tactics and procedures of on-orbit RSOs. Each individual orbital element was assessed for anomalous activity, thereby providing a higher degree of interpretability. That is to say, instead of analyzing each data observation as anomalous or not as a whole, the observations were assessed at the individual orbital element level. This provides a more in-depth understanding as to why an anomaly is determined to be one and provides deeper value provided the nature of undersupervised machine learning (ML). This type of approach can provide critical insight to establish a profile for actions indicating military activity and serving as a source of I&W. The end result demonstrates greater detail not just of anomalies in TLEs but also into which aspects of an anomalous RSO observation were dynamic.

The total number of Russian RSOs investigated was downsampled to look at the most relevant objects. The public catalog lists 25,027 Russian RSOs, a large portion of them being classified as debris. This research looked only at RSOs that were in orbit during the initial time period of the Ukraine invasion. Russian RSOS include d int eh analysis were filtered according to three selection criteria: (1) ownership classification as ”CIS” (Russian), (2) object type designated as non-debris (satellite, payload, or unknown), and (3) had a TLE observation in the public catalog between February - April 2022. This reduced the number of RSOs to 2,544 total objects for further investigation. Five models were compared for anomaly detection; isolation forest (IF) [13], autoencoder (AE) [17, 9], variational autoencoder (VAE) [11], Kolmogorov Arnold Network (KAN) [14], and a novel autoencoder approach that leverages an anchor-based loss function as a regularization term combined with reconstruction error inspired by Beta VAE (Anchor AE)[23]. Outliers were assessed for each orbital element of each RSO and used to provide true positive labeling of TLE observations to annotate data as anomalous or not. This was used to assess the performance of the ML models. While these more advanced anomaly detection methods (IF, AE, VAE, KAN, & Anchor AE) capture a wider net of anomalies than only outliers, it is assumed in this work that outliers will be flagged as anomalous by the ML approaches. With this in mind, true positive and false negative results were used as the key metric in evaluating

performance through F1 scores of the models.

The main objective of the project is to identify anomalies and detect changes in on-orbit activity during the leadup period, which is the six-month window (August 24, 2021–February 24, 2022) directly prior to the invasion of Ukraine. The timeframe used for training data that captures "normal" on-orbit activity for Russian RSOs is a 5-year sample (August 24, 2016 – August 23, 2021) preceding the leadup period. Hypothesis testing is performed using a baseline period 12–6 months prior to invasion and comparing the anomaly rate to the leadup period, 6 months directly prior. The overall findings lean in favor of supporting the alternate hypothesis of confirming unique Russian RSO activity that is outside of expected PoL/PoB. This is emphasized by an increase of 176.25% in the assessed anomaly rates between the baseline period of hypothesis testing and subsequent leadup period. This point is further driven when looking at the specific orbital elements by RSO mission class that support the alternate hypothesis. While the research strived to be comprehensive, shortcomings were faced. Anomalous activity is based only on orbital elements and does not capture changes in behavior for a wider scope of event-based activities such as maneuvers, proximity/separation, changes in attitude, or telemetry deltas. Additionally, only data made publicly available by the 18th Space Defense Squadron were used.

This research provides three significant contributions to the field. First, it introduces an efficient methodology for rapidly identifying TLE data relevant to pre-combat activity. Second, it establishes a comprehensive tactical and procedural profile of Russian military space operations prior to conflict. Third, it develops a novel anchor-loss based autoencoder architecture that demonstrates improved performance compared to existing deep learning approaches.

2. RELATED WORK

Deep learning for orbit prediction is an area that has been previously studied, researchers investigated on-board ML models to predict a vehicle's position in the absence of Global Navigation Satellite System (GNSS) signals [3]. Additional research highlights the use of an encoder-decoder structure for anomaly detection in various fields. Tan et al. implemented an encoder-decoder to detect anomalies on sequential image sensing data using real-world Additive Manufacturing data[19]. Other research used an encoder-decoder generative adversarial network (GAN) for detecting multivariate anomalies in telemetry data[22]. The general approach of using encoding-decoding and reconstruction errors for anomaly assessment has been well researched. We apply that same general methodology to anomaly detection of Russian satellite ephemeris data.

Recent advances in deep learning for anomaly detection have demonstrated the effectiveness of combining anchor-based loss functions with reconstruction-based approaches and sophisticated regularization techniques. Anchor-based methods, particularly those employing triplet loss, have emerged as powerful tools to learn discriminative feature representations that enhance anomaly detection performance. Notable implementations include the work by Tayeh et al.[20], which utilizes deep residual-based triplet networks for industrial surface anomaly detection, where defective training samples are synthesized from normal data using random erasing techniques to learn robust similarity metrics between normal and anomalous samples. Similarly, Biradar et al. [4] developed a triplet-set feature proximity learning approach for video anomaly detection that employs both normal-normal-abnormal (n-n-a) and abnormal-abnormal-normal (a-a-n) triplet configurations to encode deep features. These approaches demonstrate that triplet loss functions, with their anchor-positive-negative sample relationships, can be successfully integrated with autoencoder architectures where reconstruction loss serves as the primary anomaly detection mechanism while triplet loss enhances feature discrimination.

The integration of regularization terms in anomaly detection loss functions has proven crucial for improving model robustness and preventing overfitting to normal data patterns. Variational autoencoders (VAEs) with beta regularization represent a significant advancement, where the Evidence Lower Bound (ELBO) incorporates both reconstruction loss and weighted KL divergence terms to balance reconstruction accuracy with latent space regularization[23]. Support Vector Data Description (SVDD) represents the foundation approach, constructing minimum-volume hyperspheres that surround normal samples in features space to serve as anchors for anomaly detection [10]. Deep SVDD extends this framework by combining neural networks for feature extraction whit SVDD's hypersphere-based objectives[18].

3. METHODOLOGY

This research develops and evaluates multiple anomaly detection approaches for Russian-owned RSO orbital ephemeris data to identify potential conflict escalation indicators. The study compares a baseline isolation forest (IF) method against advanced deep learning models: simple autoencoder (AE) [5], variational autoencoder (VAE), [11], Kolmogorov Arnold Network (KANs) [14], and a novel anchor-loss based autoencoder (Anchor AE) that combines reconstruction errors with latent space geometry distances for a combined loss function. Systematic hyperparameter tuning frameworks were employed to compare and contrast the results of the various models and to ensure a comprehensive approach.

3.1 Data Preprocessing

The models rely on three primary datasets: TLEs, satellite catalog (SATCAT), and RSO mission class categorization. The TLE and SATCAT data were accessed through space-track.org [2]. TLEs were selected because they are readily available and provide a suitable historical background. They also provide the added benefit of being easily understood and act as a default standard for ephemeris data. The RSO mission class data was sourced from two separate repositories; the NASA Space Science Data Coordinated Archive (NSSDCA) [16] was the primary and supplemented by the Union of Concerned Scientists (UCS) database [21]. The training data was cleaned and filtered to control for RSOs that did not have an adequate amount of TLE observations and further downsampled to a relevant timeline applicable to the Russian invasion dates and to meet additional criteria:

1. Russian owned object annotated as “CIS” in the Space-Track satellite catalog
2. Object type of “Satellite”, “Payload”, or “Unknown” (excluding ”Debris”)
3. Observed a recorded TLE in the public catalog during the time window of February - April 2022

The data was controlled to focus on RSOs that had the potential to correlate to pre-conflict events, this was implemented by filtering out debris RSOs and RSOs that did not have a recorded TLE observation between February - April 2022. This was used to control for data samples that did not provide relevant information during the time of interest with the Russian-Ukraine invasion. After preprocessing, the data consist of selected features essential for anomaly analysis. The input features to the models were the six orbital elements contained within the TLE data samples; mean motion, eccentricity, inclination, right ascension of the ascending node (RAAN), argument of perigee, and mean anomaly.

3.2 Model Architectures

Anomaly detection was performed and compared across the five different model architectures; IF, AE, VAE, KAN, and Anchor AE. The nature of this research called for unsupervised learning in the development of each model but required a method of grounding the work to a degree of truth. To accomplish this, outliers were used as a baseline anomaly flag and assessed for each orbital element of a given RSO. Deep learning anomaly detection methods are capable of identifying anomalous observations beyond outliers and are generally understood to detect deeper linear and nonlinear relationships [6, 7, 15]. They have demonstrated the ability to capture more nuanced subtleties in distributions such as point, contextual, collective, behavioral, or structural anomalies. An assumption in this research was made to anticipate that in cases where an outlier is detected, an anomaly will also be detected by the ML approaches. That is, we assumed that in cases where an outlier occurs, the perfect model would also mark that data point as anomalous. The ideal performance would accurately predict all true positives (TP), outlier=1/anomaly=1, and have no false negatives (FN), outlier=1/anomaly=0. F1 score was used as the primary evaluation metric because it captures the balance between TP and FN. Outliers are defined in context of their interquartile range, outlier if:

$$x < Q_1 - 1.5 \times \text{IQR} \quad \text{or} \quad x > Q_3 + 1.5 \times \text{IQR}$$

Similar to how anomalies are detected within each observation by the individual orbital elements, as are outliers. Outliers were assessed by each RSOs individual orbital element and annotated as the ground truth label. For example, each orbital element for RSO Cosmos 2538 (NORAD ID 44424) was subsetted from the larger dataset and evaluated for outliers individually so when an outlier is annotated for a given orbital element such as eccentricity, it represents an outlier for the given RSO within that data of that specific orbital element. This process was applied for each individual

RSO to cover the entire dataset; this same framework was also used to predict anomalies. Each model underwent hyperparameter tuning using a grid search across a range of variables. Hyperparameter tuning was limited to a select number of RSOs due to computational restraints.

Table 1: Hyperparameter Search Configuration

Model	**Parameter Configuration**
AE	latent_dim: [2, 3, 4, 5], epochs: [100, 150, 200], batch_size: [16, 32, 64], threshold_sigma: [1.5, 2.0, 2.5]
VAE	hidden_dim: [16, 32, 64], latent_dim: [2, 3, 4, 5], epochs: [100, 150, 200], batch_size: [16, 32, 64], threshold_sigma: [1.5, 2.0, 2.5]
KAN	hidden_feat: [32, 64], grid_feat: [25, 50], num_layers: [2, 3], epochs: [100, 150], dropout: [0.3, 0.5], learning_rate: [0.001, 0.01, 0.1]
Anchor AE	hidden_dim: [16, 32, 64], latent_dim: [2, 3, 4, 5], epochs: [100, 150, 200], batch_size: [16, 32, 64], threshold_sigma: [1.5, 2.0, 2.5]
IF	contamination: [0.05, 0.1, 0.15, auto], n_estimators: [50, 100, 200], max_samples: [0.5, 0.8, 1.0]

Following hyperparameter optimization, the models were evaluated across varying temporal training windows using the optimal parameters on the full dataset containing all 2,544 Russion RSOs. Given the highly dynamic nature of the expanding space domain and its evolving operational patterns, we hypothesized that anomaly detection performance would vary significantly with training period duration. Systematic evaluation across multiple time intervals (1-5 years) was conducted to determine optimal temporal scope for each model architecture. The results demonstrated that the Anchor AE achieved the best performance with an F1 score of 0.764 when trained on a 4-year temporal window using the following hyperparameters: batch size = 16, epochs = 150, hidden dimension = 16, latent dimension = 5 and threshold $\sigma = 1.5$.

Table 2: Performance Comparison of Anomaly Detection Models

Time Period	**IF**		**AE**		**VAE**		**KAN**		**Anchor AE**	
	Acc	**F1**	**Acc**	**F1**	**Acc**	**F1**	**Acc**	**F1**	**Acc**	**F1**
5 year	0.803	**0.751**	0.654	0.674	0.634	0.657	0.773	0.680	0.744	0.749
4 year	0.813	0.758	0.650	0.679	0.642	0.677	0.808	0.730	0.756	**0.764**
3 year	0.807	**0.756**	0.623	0.645	0.610	0.638	0.786	0.697	0.706	0.722
2 year	0.727	0.650	0.639	0.645	0.580	0.588	0.712	0.601	0.711	**0.705**
1 year	0.534	0.413	0.447	0.424	0.521	**0.500**	0.527	0.368	0.522	0.482

3.3 Anchor-Loss Based Autoencoder

The Anchor AE model uses a symmetric encoder-decoder architecture. The encoder compresses the input TLE features through a series of fully connected layers with progressive dimensionality reduction. Each layer incorporates normalization and uses a leaky ReLU activation function ($\alpha = 0.2$). The decoder mirrors this structure in reverse, reconstructing the original input form the compressed latent representation. The architecture utilizes a bottleneck design where the latent space dimensionality is smaller than the input space; 6 to 5 as discovered during hyperparameter tuning. This compression forces the model to learn efficient representations of normal orbital behavior patterns, making anomalies detectable through reconstruction quality and latent space geometry.

A key aspect of the Anchor AE is the anchor-based loss function. It is a hybrid loss function that combines traditional reconstruction loss with a novel anchor-based regularization term.

$$L_{\text{total}} = L_{\text{reconstruction}} + \lambda \cdot L_{\text{anchor}} \tag{1}$$

Where:

- $L_{\text{reconstruction}} = \text{MSE}(x, \hat{x})$ captures the standard reconstruction quality
- L_{anchor} enforces structured clustering in the latent space based on k-nearest neighbor relationships
- $\lambda = 0.1$ balances the two loss components

The anchor loss is computed as:

$$L_{\text{anchor}} = \frac{1}{N}\sum_{i} \text{mean}(d(z_i, \text{NN}_k(z_i))) \tag{2}$$

Where $d(z_i, NN_k(z_i))$ represents the distances from each latent vector z_i to its k=3 nearest neighbors in the latent space. This formulation encourages the formation of compact clusters for normal data points while isolating anomalies.

There are two complimentary principles in the Anchor AE model; reconstruction based detection and latent space geometry. The reconstruction based detection identifies anomalies when observations reconstruction score surpasses the threshold sigma of 1.5, this variable being determined through hyperparameter tuning. As the model is trained on a 4-year temporal scope assumed to be normal behavioral period, there is an expected distribution that each orbital element will fall within. The nuances are encoded into the model and reflected by lower reconstruction values. As anomalies are presented to the model, the reconstruction values that increase beyond threshold are flagged. The other side of the Anchor AE loss function is the latent space geometry. The anchor loss term provides regularization and structures the latent space such that normal samples form tight clusters. Anomalous samples are pushed away from these clusters and exhibit larger distances from their nearest neighbor and have higher isolation scores. This dual principle approach provides a more robust anomaly detection framework by leveraging both the representational capacity of autoencoders and the geometric properties of embedding spaces. The method is well suited for use cases where normal operational patterns have consistent physical constraints.

4. EXPERIMENT SETUP

The experiments aim to evaluate the effectiveness of the various approaches for detecting anomalies in orbital patterns, specifically focusing on the ability to identify patterns focused on a country's activity during an escalation to conflict. All methods are tested on orbital TLE data, focusing on the six classical orbital elements because of the relevancy they have to potential maneuvers or irregular movements.

The Anchor AE model was chosen based on evaluation metrics and model performance. It was the method used to train and perform inference on the full inference dataset. The model parameters were determined based on a grid search hyperparameter tuning process using the configuration described above in Table 1. This step was critical in providing a fair assessment across the different anomaly detection methods and optimizing model performance. The interquartile range was used in all cases to identify outliers within each observation to serve as the ground truth labels. An Anchor AE model was trained using the above-described framework for each Russian space object, in total 2,544 models were trained using the training dataset of Russian RSO TLE observations. Once a baseline of normal behavior was established and learned by the model, new data was introduced to assess anomalous activity at inference using TLE data observations.

The initial training dataset consisted of 5 years of TLE data ranging from August 24, 2016 to August 23, 2021. With the invasion date being February 24, 2022, this research assumed a 6-month window for leadup time where potential anomalous behavior was likely to occur. Tuned models were further assessed for performance on various temporal windows to find the best suited training data window. As noted in Table 2 a 4-year temporal window, August 24, 2017 to August 23, 2021, demonstrated the best performance for the AE Anchor model. The data used for inference to investigate anomalous behavior was divided into two time periods; 1) lead up is the 6-month period prior to Ukraine invasion (August 24, 2021 – February 24, 2022) and 2) post-invasion is February 24, 2022, to February 24, 2024. In addition, a different leadup period was established for hypothesis testing. Hypothesis testing was conducted using the 12-month period directly prior to the invasion date. The time period ranging from February 24, 2021 to August 23, 2021 was used as the hypothesis testing baseline period with the leadup period remaining the same (August 24, 2021 to February 24, 2022).

4.1 Hypothesis Testing

The hypothesis testing was conducted by separating the 12 months directly prior to the invasion date into a baseline and investigation period. The first 6-month window, February 24, 2021 to August 23, 2021, was the baseline period used for hypothesis testing and the second 6-month window, August 24, 2021 to February 24, 2022, was used as the investigative or leadup period. The null and alternate hypotheses were established and used a standard significance level ($\alpha = 0.05$).

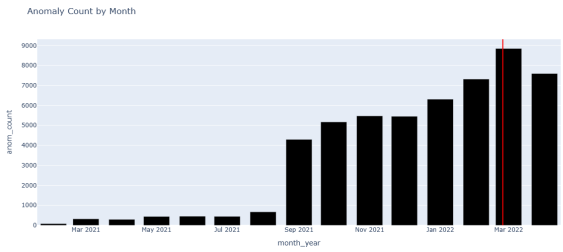

Fig. 2: Total anomalies assessed by month

- **Null Hypothesis (H_0):** No meaningful change in Russian RSO activity that is outside of expected Pattern of Life/Pattern of Behavior
- **Alternate Hypothesis (H_1):** Existence of meaningful change in Russian RSO activity that is outside of expected Pattern of Life/Pattern of Behavior

Hypothesis testing revealed statistically significant evidence supporting the alternate hypotheses. A chi-square test of independence was conducted to compare anomaly rates between the hypothesis testing baseline period and the leadup period. The analysis yielded a chi-square statistic of $\chi^2 = 21,276.23$ with a p-value of effectively zero ($p < 0.001$). These results provide overwhelming evidence to reject the null hypothesis at the significance level $\alpha = 0.05$. Furthermore, the anomaly rate between the baseline and leadup periods dramatically increased from 0.19% to 3.01%, a 15.8-fold increase. The contingency analysis showed:

- **Baseline period:** 1,634 anomalies out of 842,269 total observations
- **Lead-up period:** 26,536 anomalies out of 880,546 total observations

These findings demonstrate strong statistical evidence ($p < 0.001$) for meaningful change in Russian RSO on-orbit activities during the six months preceding the invasion, thereby supporting the alternate hypothesis that anomalous orbital behavior significantly exceeded expected PoL/PoB.

5. RESULTS AND FINDINGS

5.1 Pattern of Overall Anomalies

The analysis assessed anomalies in each orbital element for individual RSOs. TLE data for each object–such as Cosmos 2532 (NORAD ID 43753)–was subsetted from the larger dataset for inference. The individual orbital elements were then examined for anomalous observations by specific RSO. This method was repeated for all RSOs thereby looking at RSO specific behaviors with a unique model trained and encoded to each. When an observation for any given orbital element was flagged as an anomaly the entire observation was then counted as anomalous at the aggregated level. Even in cases where more than one orbital element was anomalous, the observation was simply marked as an anomaly because one or more of the orbital elements was assessed as such.

While the overall total detected anomalies dramatically increased in the 6-month window preceding the invasion date, the first notable increase occurred in August and was followed by a massive increase in anomalies in September 2021 (6 to 5-months prior). September 2021 had 4,297 detected anomalies up from 671 the month prior, this represents a 504% increase. The following months leading up to February 2022 had a progressive increase in the number of anomalies, demonstrating the statistical significance of the model findings.

Understanding anomalies at this high level provides a primary advantage in quickly assessing on-orbit activity and flagging the observation for further investigation. Considering the large number of RSOs and the massive volume of data, this method provides a framework for rapidly identifying points of interest. Essentially, it serves as a quick way to find ”the needle in the haystack” but does not provide granular details related to the anomalous occurrence. Digging further into the identified anomalies provides a deeper understanding of on-orbit activities in regards to potential pre-combat tactics and procedures.

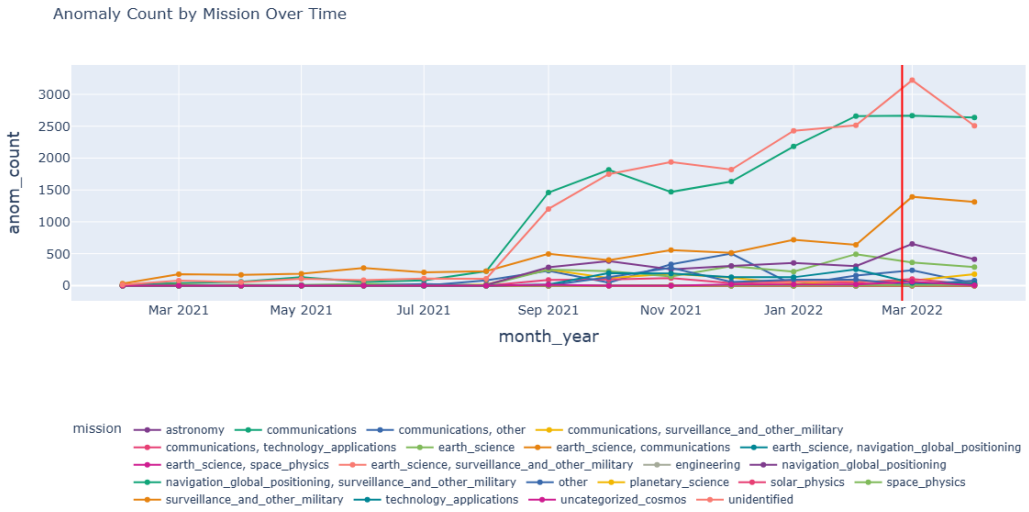

Fig. 3: Total anomalies assessed by RSO mission during the leadup period

5.2 Pattern of Anomalies by Mission

The findings indicate a statistically significant spike in anomalies for RSOs in the mission class communication and unidentified. These two categories of RSO have the highest number of anomalies and begin violating PoL/PoB in August-September timeframe. It should be noted that these two categories also make up the largest two mission classes of Russian RSOs with communication RSOs representing 31.46% and unidentified RSOs representing 37.96%. Communication satellites are unique in a small number being classified as joint use (for example: communication and surveillance/other military, communication and other, communication and technology applications). The rapid increase in anomalies for communication and unidentified RSOs represents a significant shift in operations and can represent the importance of these mission classes to military operations. Subsequently, there is also a notable increase

Table 3: Russian Mission Distribution of Communication RSOs

Mission Type	**Count**	**% Total of all RSOs**	**% Comms RSOs**
Communications	1,411,466	29.85%	94.40%
Comms, surveillance & military	50,499	1.07%	3.38%
Comms, other	20,957	0.44%	1.40%
Comms, technology applications	7,084	0.15%	0.47%
Earth science, communications	5,180	0.11%	0.35%
Total	**1,495,186**	–	**100.00%**

in anomalies for RSO mission classes navigation global positioning and surveillance & other military. These two mission classes of RSO, while also demonstrating significant increase in anomalies, follow a much different pattern than communication and unidentified mission classes. There is a far more gradual and progressive growth starting around September and incrementally increasing through February. Similar to communication, this finding stands out because of the importance navigation and surveillance have in military operations.

5.3 Pattern of Anomalies by Orbital Element

This study prioritized interpretability by analyzing individual orbital elements for anomalous activity, enabling identification of specific changes within each observation that constitute anomalous behavior. This provides a deeper understanding of potential tactics and procedures leading up to a large military action. The analysis examines how RSOs moved during the leadup period, focusing on objects with a mission class of communications, navigation global positioning, surveillance and other military, and unidentified. Anomalous activities are evaluated from two complementary perspectives: temporal variations time series data and distributional characteristics of orbital change. The former provides a detailed look what occurred during the leadup time while the later establishes a high level profile of operational patterns.

Individual orbital element dynamics were averaged by mission class and compared using the baseline period of February 24, 2021 to August 23, 2021 and the leadup period of August 24, 2021 - February 24, 2022. This provides distinct insight into how mission classes were leveraged and the means by which they were moved.

Table 4: Percent Change by Mission Type and Orbital Elements Comparing Baseline to Leadup

Mission Type	Inclination	RAAN	Eccentricity	Arg of Perigee	Mean Anomaly	Mean Motion
Communications	39%	-201%	-154%	-123%	-277%	-16%
Navigation	-165%	-172%	-161%	2%	-158%	-165%
Surveillance	93%	-273%	-803%	-615%	-809%	-332%
Unidentified	64%	-202%	-301%	-145%	-193%	-435%

Communication RSOs demonstrated a decline in eccentricity with the average reaching its lowest point in February, 2022. There was also an overall increase in RAAN when comparing the baseline and leadup periods. Further analysis revealed strong correlations between pairings of orbital elements for communication RSOs broken out into orbital regime.

- LEO - eccentricity & inclination: -0.75, RAAN & mean anomaly: 0.77
- MEO - eccentricity & mean motion: -0.91, eccentricity & arg of perigee: -0.97, inclination & RAAN: -0.9
- GEO - mean motion & eccentricity: 0.89

Navigation global positioning RSOs had a shared decline in eccentricity and mean motion starting in September/October 2021 accompanied by a large increase in RAAN. Additionally, within a similar time window there were noticeable spikes in argument of perigee (November, 2021) and mean anomaly (December 2021). Correlated patterns were also observed for this RSO mission class:

- LEO - inclination & mean motion: -0.78, mean anomaly & arg of perigee: 0.67
- MEO - eccentricity & mean anomaly: 0.81, RAAN & eccentricity: 0.84

Surveillance and other military RSOs generally appeared to have a higher degree of non-uniform changes. Mean motion witnessed a rapid increase starting in November 2021 following a general decline in the preceding months. There was also a large decrease in mean anomaly in January 2022 accompanied by a spike in argument of perigee. Eccentricity also rapidly dropped in November 2021 and remained low through February 2022. Correlated pairings for surveillance and other military RSOs were assessed:

- LEO - eccentricity & mean motion: 0.86
- MEO - arg of perigee & inclination: 0.99, RAAN & mean motion: -0.72
- GEO - inclination & mean anomaly: -0.61, eccentricity & RAAN: 0.81, mean motion & RAAN: -0.72

RSOs with an unidentified mission class are the most non-uniform in terms of changes between the baseline and leadup. This is primarily theorized to be attributed to the diverse purposes and mission classes potentially captured within this category. However, there are some specific observations of interest. There is a distinct decrease in mean motion and inclination that occurs nearly simultaneously in December 2021 immediately followed by a rapid increase in these two orbital elements. Additionally, there is an overall increase in RANN witnessed between the two temporal windows. Assessing correlation patterns shows further understanding.

- LEO - inclination & arg of perigee: -0.52
- MEO - inclination & mean motion: -0.89, inclination & mean anomaly: -0.71, inclination & eccentricity: 0.85, eccentricity & mean motion: -0.98

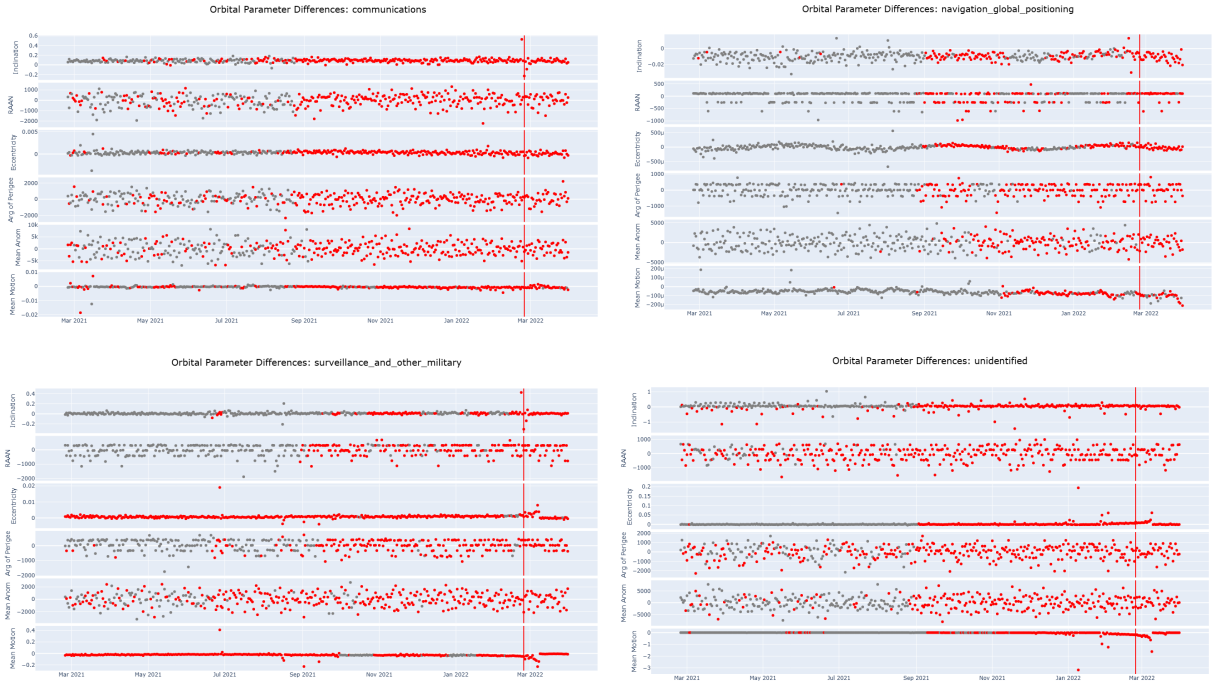

Fig. 4: Differences between observations demonstrating the rate of change for each orbital element by mission type. Anomalous observations are marked as red.

The overall dynamics of the RSOs are evident when analyzing the individual orbital elements from at an aggregated level. Rather than examining absolute measures, this analysis focused on observation-to-observation changes in anomalous data during the leadup period. A differencing approach assessed changes between each observation and its previous data point (X_T-X_{T-1}) for each orbital element by individual RSO. The analysis then examined anomalous observations to understand how these data points deviated from their last know state.

Fig. 6 captures a high-level picture of differences between observations for anomalies. This approach assessed the total changes between anomalies and their most recent observations, quantifying the degree of change for each orbital element. The results reveal potential tactical patterns across Russia's space assess with plots highlighting a notable shift in operations occurring 6 to 5 months prior to February 2022.

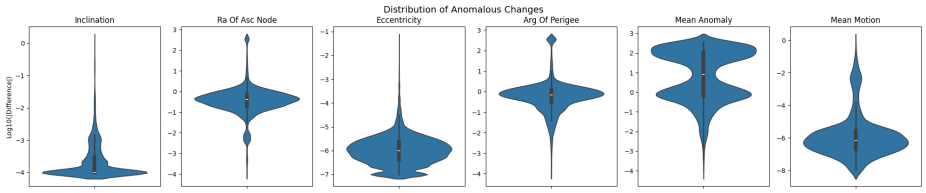

Fig. 5: Distribution of changes for anomalous observations between X_T and X_{T-1}

In an attempt to further roll up this analysis, an aggregated analysis was performed to capture the differences in anomalous observations. Fig. 5 captures the distribution of changes observed for anomalies and each previous observation. This analysis was performed for the leadup period and captures the total distribution of changes in each orbital element.

One specific finding in the data is around the RSO mission class "technology applications". While this mission class is relatively small, there are distinct anomalous patterns detected starting in September 2021 with increases to inclination

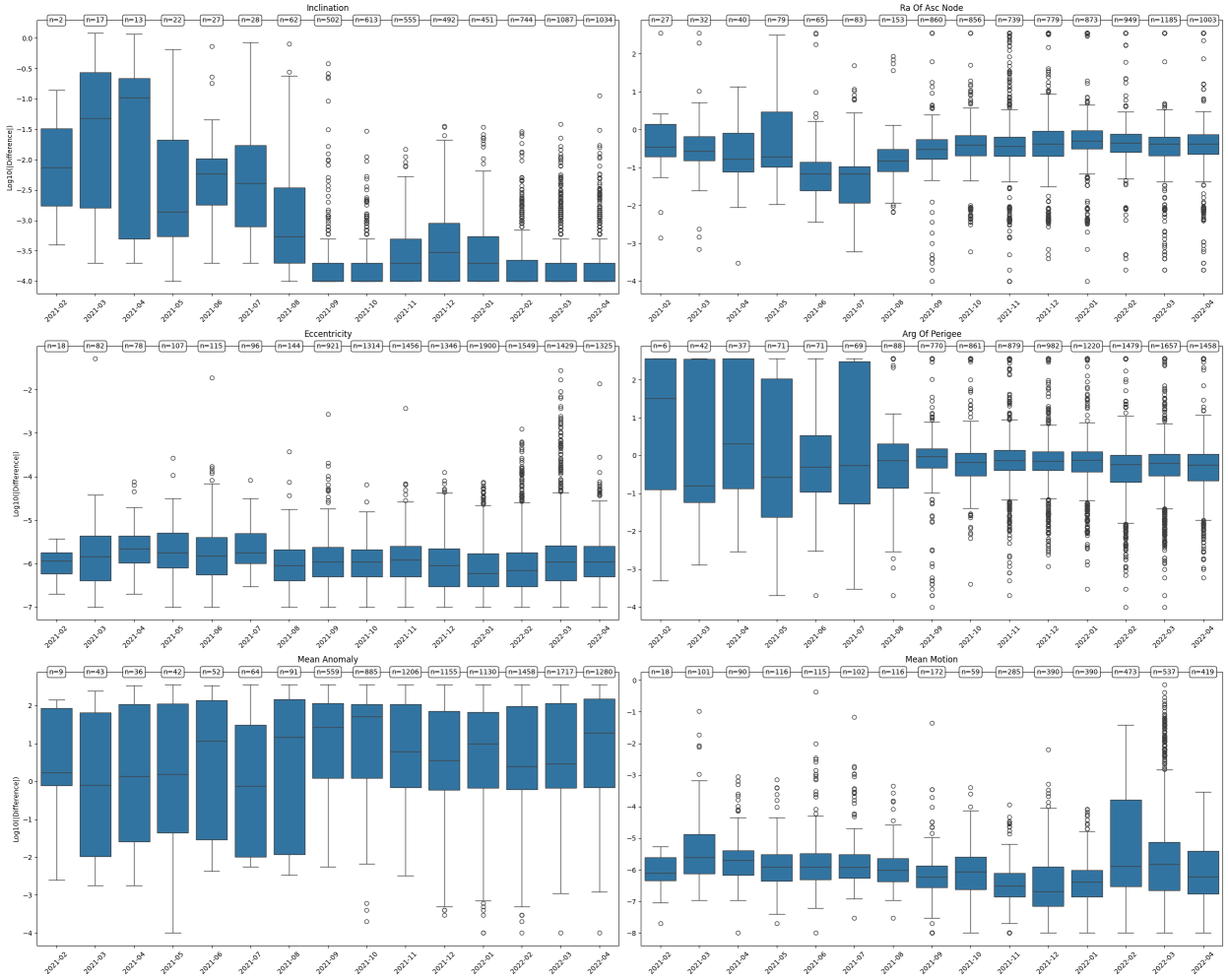

Fig. 6: Distribution and outlier assessment of differences observed within each orbital element

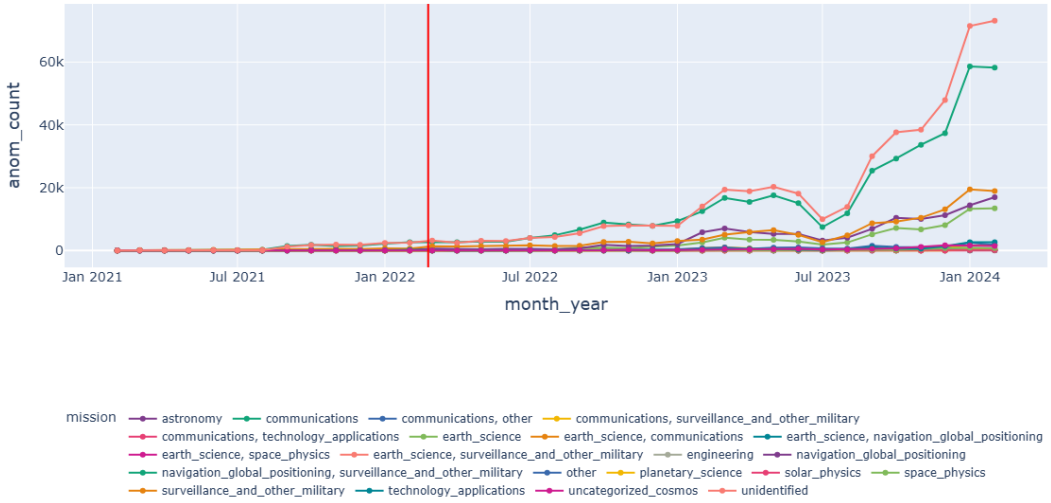

Fig. 7: Total anomaly counts by mission class post invasion timeline

and ending in a steep drop off in March 2022. In particular, it shows a very rapid increase in mean motion directly leading up to the invasion date and carrying into the early part of March. While the underlying purpose or meaning behind this is unknown, it is a distinct finding in the analysis that stands out because of its rapid and isolated behavior. This type of pattern can be used to flag for further investigation. For example, the anomalous behavior witnessed in mission class "technology applications" is primarily attributed to the RSO SAMSAT 218D (NORAD ID: 41466). Performing an open search for this RSO shows that it is a cube satellite developed by the Samara State Aerospace University (SSAU). It serves as an educational satellite used for testing "algorithms for controlling the orientation of nano-satellites" [12, 1]. While this specific satellite serves educational purposes, it demonstrates how the type of research outlined in this study can be used to quickly identify potential objects of interest that warrant further investigation.

5.4 Post Invasion

The total number of anomalies and subsequent findings by mission class can serve as potential I&W of future conflicts. The research and the findings of this study demonstrate strong statistical significance for increasing violations of PoL/PoB by Russian RSOs in the 6 months preceding the Ukraine invasion. To further support this claim, an analysis of post invasion on-orbit behavior reveals not only a continuation of anomalies but also shows exponential growth in the number of anomalies. In the months and years following February 24, 2022, the rate of anomalies rapidly expands to the point of overshadowing the leadup period anomaly rates. Looking beyond the leadup timeframe reveals that patterns identified within it not only continue but overwhelmingly grow in terms of scope and occurrence. The anomaly rate in the 6-month leadup period is 3.01%, as operations transition into a post-invasion posture the anomaly rate between February 25, 2022 to February 24, 2024 increases to an overwhelming 27.83%. Furthermore, the RSO mission classes that were the largest violators of PoL/PoB during the leadup period(i.e. communication, surveillance & other military, navigation global positioning, and unidentified), are the exact same mission classes with the highest number of anomalies during the post invasion timeframe. These findings support the established pattern from the leadup period and further contribute to establishing a pre-combat profile of Russian space operations. Additionally, RSOs with a mission class of "earth science" show a significant increase in anomalies post invasion, with anomalies increasing in the September/October 2022 timeframe. This pattern in "earth science" RSOs continues to progressively grow into February 2024.

The documented escalation from 3.01% to 27.83% anomaly rates represents more than statistical significance - it demonstrates a fundamental transformation in space-based operations supporting terrestrial conflict. This pattern suggests that space assets have become increasingly central to military operations, moving from supporting roles to primary operational platforms. The sustained nature of these elevated anomaly rates, coupled with the expansion into previously stable mission classes like "earth science", indicates that space-based military operations may have become normalized rather than exceptional. This normalization carries significant implications for future conflict prediction, as

similar patterns of escalation may serve as reliable indicators of impending military action in other regions or contexts. This serves to support the central idea that analyzing RSO behaviors can provide a credible source to complementing and enhancing military intelligence. The integration of space-based data science behavioral analysis into existing intelligence frameworks represents a force multiplier for national security agencies. The physical constraints of orbital mechanics mean that significant changes in space-based operations inevitably leave detectable signatures.

6. FUTURE WORK

Future work following this research can expand deeper into the development of a pre-combat profile. Further investigation can be performed to better understand changes in orbital activity. The number of real-world instances where large scale military conflict operations taken by space-enabled nations is limited. However, there are other instances where a similar analysis can be performed to compare results. Finding additional scenarios to analyze would help to further establish or refute the patterns assessed within this study. While real-world examples are preferred from an analytical and scientific perspective, it is certainly good that there are not a lot of real-world, large-scale conflict examples. As an alternative, this analysis can be applied to military exercises with a particular focus on exercises that include distinct military space-based support to terrestrial effects. This option provides the best path forward to contributing evidence of the effectiveness of this research.

Research could also expand by continuing the development on novel anomaly detection methods. Space-related data, and many other fields, have a common problem of small to nil anomalies. This creates a large imbalance in training data and at times, anomalies are naturally occurring because of the space environment or from calibration issues with sensors. Developing more advanced anomaly detection methods that are specifically tailored to deal with challenges of the space domain would greatly expand downstream effects.

7. REFERENCES

[1] Samsat-218d. `https://nssdc.gsfc.nasa.gov/nmc/spacecraft/display.action?id=2016-026C`, 2016. Accessed: 2025-08-21.

[2] 18th Space Defense Squadron. Space-track.org. `https://www.space-track.org/`, 2025. Space Situational Awareness Data Repository.

[3] T. S. Bae, M. H. Kim, M. S. Kim, and S. H. Lim. Real-time Orbit Prediction based on Deep Learning. In *AGU Fall Meeting Abstracts*, volume 2019 of *AGU Fall Meeting Abstracts*, pages G21C–0753, December 2019.

[4] Kuldeep Marotirao Biradar, Murari Mandal, Sachin Dube, Santosh Kumar Vipparthi, and Dinesh Kumar Tyagi. Triplet-set feature proximity learning for video anomaly detection. *Image and Vision Computing*, 150:105205, 2024.

[5] Roel Bouman and Tom Heskes. Autoencoders for anomaly detection are unreliable. 2025.

[6] Guilherme O. Campos, Arthur Zimek, Jörg Sander, Ricardo J. G. B. Campello, Barbora Micenková, Erich Schubert, Ira Assent, and Michael E. Houle. On the evaluation of unsupervised outlier detection: measures, datasets, and an empirical study. *Data Mining and Knowledge Discovery*, 30(4):891–927, July 2016.

[7] Guilherme O. Campos, Arthur Zimek, Jörg Sander, Ricardo J. G. B. Campello, Barbora Micenková, Erich Schubert, Ira Assent, and Michael E. Houle. On the evaluation of unsupervised outlier detection: Measures, datasets, and an empirical study [supplementary material]. `[INSERT_URL_HERE]`, 2016. Supplementary material for: Data Mining and Knowledge Discovery 30(4): 891-927, 2016, DOI: 10.1007/s10618-015-0444-8.

[8] Karli Goldenberg. War in the final frontier: Space enables army operations, ensures future success. *AUSA News*, June 2024.

[9] Simon Hawkins, Haibo He, Graham Williams, and Rohan Baxter. Outlier detection using replicator neural networks. *Data warehousing and knowledge discovery*, pages 170–180, 2002.

[10] Renxue Jiang, Zhiji Yang, and Jianhua Zhao. A complete deep support vector data description for one class learning. *IEEE Access*, 11:117494–117507, 2023.

[11] Diederik P. Kingma and Max Welling. An introduction to variational autoencoders. *Foundations and Trends® in Machine Learning*, 12(4):307–392, 2019.

[12] Gunter Dirk Krebs. Samsat-218d. `https://space.skyrocket.de/doc_sdat/samsat-218d.htm`, 2024. Accessed: 2025-08-21.

[13] Fei Tony Liu, Kai Ming Ting, and Zhi-Hua Zhou. Isolation forest. In *2008 eighth ieee international conference on data mining*, pages 413–422. IEEE, 2008.

[14] Ziming Liu, Yixuan Wang, Sachin Vaidya, Fabian Ruehle, James Halverson, Marin Soljačić, Thomas Y. Hou, and Max Tegmark. Kan: Kolmogorov-arnold networks. 2025.

[15] Shanay Mehta, Shlok Mehendale, Nicole Fernandes, Jyotirmoy Sarkar, Santonu Sarkar, and Snehanshu Saha. Benchmarking anomaly detection algorithms: Deep learning and beyond, 2025.

[16] NASA Space Science Data Coordinated Archive. Nasa space science data coordinated archive. `https://nssdc.gsfc.nasa.gov/`, 2025. NASA's archive for space science mission data.

[17] Asif Ahmed Neloy and Maxime Turgeon. A comprehensive study of auto-encoders for anomaly detection: Efficiency and trade-offs. *Machine Learning with Applications*, 17:100572, 2024.

[18] Manuel Pérez-Carrasco, Guillermo Cabrera-Vives, Lorena Hernández-García, Francisco Forster, Paula Sánchez-Sáez, Alejandra Muñoz Arancibia, Nicolás Astorga, Franz Bauer, Amelia Bayo, Martina Cádiz-Leyton, and Marcio Catelan. Multi-class deep svdd: Anomaly detection approach in astronomy with distinct inlier categories, 2023.

[19] Yingshui Tan, Baihong Jin, Alexander Nettekoven, Yuxin Chen, Yisong Yue, Ufuk Topcu, and Alberto Sangiovanni-Vincentelli. An encoder-decoder based approach for anomaly detection with application in additive manufacturing. In *2019 18th IEEE International Conference On Machine Learning And Applications (ICMLA)*, pages 1008–1015, 2019.

[20] Tareq Tayeh, Sulaiman Aburakhia, Ryan Myers, and Abdallah Shami. Distance-based anomaly detection for industrial surfaces using triplet networks, 2020.

[21] Union of Concerned Scientists. Ucs satellite database. `https://www.ucs.org/resources/satellite-database`, January 2024. Data current through May 1, 2023. Database of 7,560 operational satellites.

[22] Zhaoping Xu, Zhijun Cheng, QiDeng Tang, and Bo Guo. An encoder-decoder generative adversarial network-based anomaly detection approach for satellite telemetry data. *Acta Astronautica*, 213:547–558, 2023.

[23] Leixin Zhou, Wenxiang Deng, and Xiaodong Wu. Unsupervised anomaly localization using vae and beta-vae, 2020.

A. APPENDIX

Table 5: Monthly Change in RSO Activity by Mission Type (Change/Percent Change) - Green cells indicate a month-over-month change in anomalies larger than the mean value

Mission Type	**2021-07**	**2021-08**	**2021-09**	**2021-10**	**2021-11**	**2021-12**	**2022-01**	**2022-02**
astronomy	–	–	–	–	1/100%	-1/-50%	–	-1/-100%
communications	26/47%	143/177%	1236/552%	355/24%	-346/-19%	163/11%	550/34%	478/22%
communications, other	-2/-100%	–	150/183%	-185/-80%	287/611%	167/50%	-493/-98%	148/1850%
communications, surveillance and other military	-2/-100%	–	234/1300%	-133/-53%	65/55%	-61/-33%	-98/-80%	36/144%
communications, technology applications	–	–	–	6/7%	22/23%	-78/-67%	32/82%	-29/-41%
earth_science	-17/-63%	-8/-80%	247/12350%	-22/-9%	-85/-37%	162/114%	-85/-28%	274/125%
earth_science, communications	–	–	–	–	5/250%	-4/-57%	3/100%	-4/-67%
earth_science, navigation global positioning	–	–	–	–	–	–	–	–
earth_science, space_physics	–	–	–	–	–	–	–	–
earth_science, surveillance and other military	–	-3/-100%	–	–	–	–	55/2750%	21/37%
engineering	–	–	–	–	–	–	–	–
navigation_global_positioning	-2/-67%	10/1000%	275/2500%	98/34%	-129/-34%	53/21%	47/15%	-50/-14%
navigation global positioning, surveillance and other military	–	–	–	–	–	–	–	–
other	23/1150%	-23/-92%	–	129/6450%	148/113%	-222/-80%	34/60%	1/1%
planetary_science	–	-2/-100%	–	–	–	–	–	–
solar_physics	–	-2/-100%	–	–	–	–	–	–
space_physics	–	-2/-100%	–	–	-3/-100%	–	–	–
surveillance_and_other_military	-67/-24%	18/9%	271/120%	-97/-20%	156/39%	-43/-8%	206/40%	-81/-11%
technology_applications	–	–	–	181/1131%	-9/-5%	-58/-31%	–	125/96%
uncategorized_cosmos	–	-1/-100%	–	-12/-100%	–	–	-3/-17%	3/20%
unidentified	23/27%	-3/-3%	1096/1034%	547/46%	190/11%	-119/-6%	609/33%	85/4%

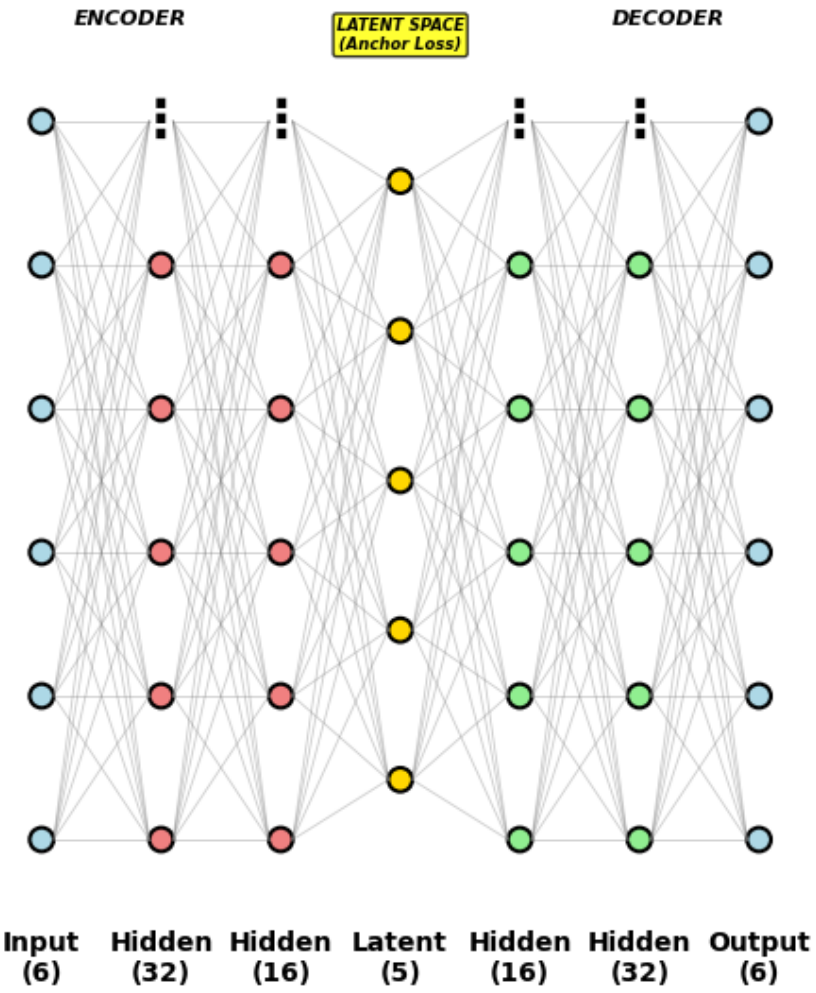

Fig. 8: Anchor AE model architecture fully connected

Fig. 9: Correlation of changes in orbital element differences by mission type

Fig. 10: Correlation of anomaly counts between orbital elements by mission type

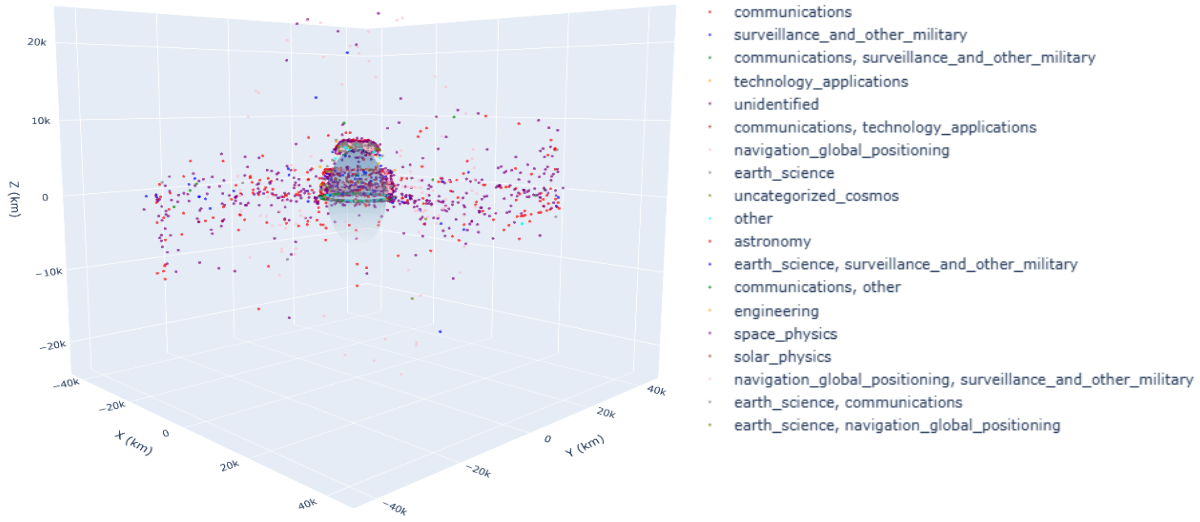

Fig. 11: Plot of anomalies observed